Analysis of CD8$^+$ T cell response during the 2013–2016 Ebola epidemic in West Africa

Saori Sakabe[a,1], Brian M. Sullivan[a,1,2], Jessica N. Hartnett[b], Refugio Robles-Sikisaka[a,c], Karthik Gangavarapu[d], Beatrice Cubitt[a], Brian C. Ware[a], Dylan Kotliar[e], Luis M. Branco[f], Augustine Goba[g,h], Mambu Momoh[g,h,i], John Demby Sandi[g,h], Lansana Kanneh[g,h], Donald S. Grant[g,h,j], Robert F. Garry[b], Kristian G. Andersen[a,c], Juan Carlos de la Torre[a], Pardis C. Sabeti[e], John S. Schieffelin[k], and Michael B. A. Oldstone[a,2]

[a]Viral-Immunobiology Laboratory, Department of Immunology and Microbiology, The Scripps Research Institute, La Jolla, CA 92037; [b]Department of Immunology and Microbiology, Tulane University School of Medicine, New Orleans, LA 70112; [c]Scripps Translational Research Institute, The Scripps Research Institute, La Jolla, CA 92037; [d]Department of Molecular and Experimental Medicine, The Scripps Research Institute, La Jolla, CA 92037; [e]FAS Center for Systems Biology, Harvard University Medical School and The Broad Institute of Massachusetts Institute of Technology, Boston, MA 02142; [f]Zalgen Labs, Germantown, MD 20876; [g]Viral Hemorrhagic Fever Program, Kenema Government Hospital, Kenema, Sierra Leone; [h]Ministry of Health and Sanitation, Freetown, Sierra Leone; [i]Eastern Polytechnic Institute, Kenema, Sierra Leone; [j]College of Medicine and Allied Health Sciences, University of Sierra Leone, Freetown, Sierra Leone; and [k]Department of Pediatrics, Tulane University School of Medicine, New Orleans, LA 70112

Contributed by Michael B. A. Oldstone, June 18, 2018 (sent for review April 13, 2018; reviewed by Arturo Casadevall and Bruce D. Walker)

The recent Ebola epidemic exemplified the importance of understanding and controlling emerging infections. Despite the importance of T cells in clearing virus during acute infection, little is known about Ebola-specific CD8$^+$ T cell responses. We investigated immune responses of individuals infected with Ebola virus (EBOV) during the 2013–2016 West Africa epidemic in Sierra Leone, where the majority of the >28,000 EBOV disease (EVD) cases occurred. We examined T cell memory responses to seven of the eight Ebola proteins (GP, sGP, NP, VP24, VP30, VP35, and VP40) and associated HLA expression in survivors. Of the 30 subjects included in our analysis, CD8$^+$ T cells from 26 survivors responded to at least one EBOV antigen. A minority, 10 of 26 responders (38%), made CD8$^+$ T cell responses to the viral GP or sGP. In contrast, 25 of the 26 responders (96%) made response to viral NP, 77% to VP24 (20 of 26), 69% to VP40 (18 of 26), 42% (11 of 26) to VP35, with no response to VP30. Individuals making CD8$^+$ T cells to EBOV VP24, VP35, and VP40 also made CD8$^+$ T cells to NP, but rarely to GP. We identified 34 CD8$^+$ T cell epitopes for Ebola. Our data indicate the immunodominance of the EBOV NP-specific T cell response and suggest that its inclusion in a vaccine along with the EBOV GP would best mimic survivor responses and help boost cell-mediated immunity during vaccination.

Ebola | virus-specific | CD8 T cells | epitopes | HLA

The West African Ebola epidemic from 2013 to 2016 exemplified how an infectious and lethal pathogen can spread uncontrolled in an immunologically naïve population. The devastation in the affected countries—Sierra Leone, Liberia, and Guinea—resulted in over 28,000 documented infections and 12,000 deaths, dislocation of families and populations, creation of large groups of orphans, and devastation of local and national economies (1, 2). These results alerted scientific communities, the World Health Organization, and other nongovernment and government agencies to draft plans and provide resources to control, prevent, or minimize future Ebola virus disease (EVD) outbreaks through the development of diagnostic tests for surveillance (3–5), antivirals for control (6–8), and vaccines for prevention (9–11).

Ebola virus (EBOV), a member of the Filoviridae family, is a highly pathogenic virus for humans (1, 2, 12). EBOV is an enveloped virus with a negative single-strand RNA genome whose seven genes encode eight proteins with the following 3′ to 5′ genome order: nucleoprotein (NP), VP35, VP40, glycoprotein (GP) and soluble GP (sGP), VP30, VP24, and L polymerase (12). The pathogenesis and human immune response to EBOV remain largely uncharacterized for several reasons. First, EBOV is a highly fatal and infectious virus that must be handled in high-containment biosafety level 4 laboratories. Second, excluding the West Africa EVD epidemic, all previous recorded outbreaks involved a limited number of cases and occurred in mostly remote parts of central Africa, where samples from infected individuals and survivors were difficult to obtain (2, 12, 13).

The immune response to any infectious agent comprises an early innate response followed by an adaptive response responsible for purging the virus, leading to clinical recovery and future protection. The humoral arm (antibodies) of the adaptive immune response functions to lower viremia through several different mechanisms, including preventing virus attachment to permissive cells and targeting free virions for destruction by phagocytic cells, which restrict virus spread to tissues or organs. EBOV-specific IgM has been detected as early as 2–3 d and IgG as early as 6 d postsymptom onset, although the latter has frequently been observed as late as the second week postsymptom onset, a time when viremia has

Significance

Zaire ebolavirus (EBOV) is a viral pathogen of significant global health concern best exemplified by more than 28,000 human infections during the recent West African epidemic. Examining immunity in EBOV disease survivors has been historically difficult due to the occurrence of only small outbreaks in remote regions of central Africa. Consequently, little data exist describing EBOV-specific T cell responses during human infection. We examined virus-specific CD8$^+$ T cell immunity in 32 Sierra Leonean survivors of the 2013–2016 epidemic. CD8$^+$ T cells against the nucleoprotein dominated the EBOV-specific responses in this group, while a minority of individuals harbored memory CD8$^+$ T cells against the EBOV-GP. Our data have implications in designing EBOV vaccines that can elicit cell-mediated immunity in a large group of individuals.

Author contributions: S.S., B.M.S., R.F.G., K.G.A., J.C.d.l.T., P.C.S., J.S.S., and M.B.A.O. designed research; S.S., B.M.S., J.N.H., R.R.-S., K.G., B.C., B.C.W., D.K., L.M.B., A.G., M.M., J.D.S., L.K., D.S.G., R.F.G., and J.S.S. performed research; S.S., B.M.S., R.R.-S., K.G., D.K., R.F.G., K.G.A., and M.B.A.O. analyzed data; and S.S., B.M.S., and M.B.A.O. wrote the paper.

Reviewers: A.C., The Johns Hopkins Bloomberg School of Public Health; and B.D.W., Ragon Institute of Massachusetts General Hospital, Massachusetts Institute of Technology, and Harvard University.

The authors declare no conflict of interest.

Data deposition: The data from this study have been deposited in the Immune Epitope Database, www.iedb.org/SubID/1000771.

[1]S.S. and B.M.S. contributed equally to this work.

[2]To whom correspondence may be addressed. Email: bsully@scripps.edu or mbaobo@scripps.edu.

This article contains supporting information online at www.pnas.org/lookup/suppl/doi:10.1073/pnas.1806200115/-/DCSupplemental.

Published online July 23, 2018.

begun to clear (14). This antibody response may be impaired in fatal cases of EBOV infection (15). The cellular arm of the adaptive immune response primarily consists of $CD8^+$ cytotoxic T lymphocytes, which specifically identify and destroy virus-infected cells, thus eliminating factories that produce progeny virus (16, 17). $CD4^+$ T cells primarily act as helper cells for $CD8^+$ T cells and B cells. Here we focus on the $CD8^+$ T cell response to EBOV proteins in naturally infected individuals who survived the disease.

The importance of cell-mediated immunity after vaccination of nonhuman primates (NHPs) has been controversial. Sullivan et al. (18), using an Ad5-based vaccine, showed that protection following lethal challenge of EBOV in NHPs depends on $CD8^+$ T cells. Deletion of $CD8^+$ T cells in vivo using a monoclonal antibody that did not affect CD4 T cells or the humoral antibody response failed to protect, while the presence of $CD8^+$ T cells resulted in survival. Furthermore, passive transfer of high titered polyclonal anti-EBOV antibodies, several-fold higher than levels associated with survival upon EBOV challenge, also failed to provide protection (18, 19). Conflicting data from Marzi et al. (20) show that $CD8^+$ T cells are dispensable for protection from lethal challenge in NHPs vaccinated with recombinant vesicular stomatitis virus (rVSV)-Zaire ebolavirus. Both vaccines employ GP as the sole EBOV immunogen. Recently McElroy et al. (14) studied the adaptive immune response during the acute phase of EBOV infection in four American healthcare workers infected in Africa and air-transported to Emory Medical Center in Atlanta, Georgia. All four survived, showed striking activation of EBOV-specific B and T cells, and generated $CD8^+$ T cell responses to EBOV proteins (14, 21). Here we analyze T cell responses to EBOV proteins, map epitopes within those proteins, and provide

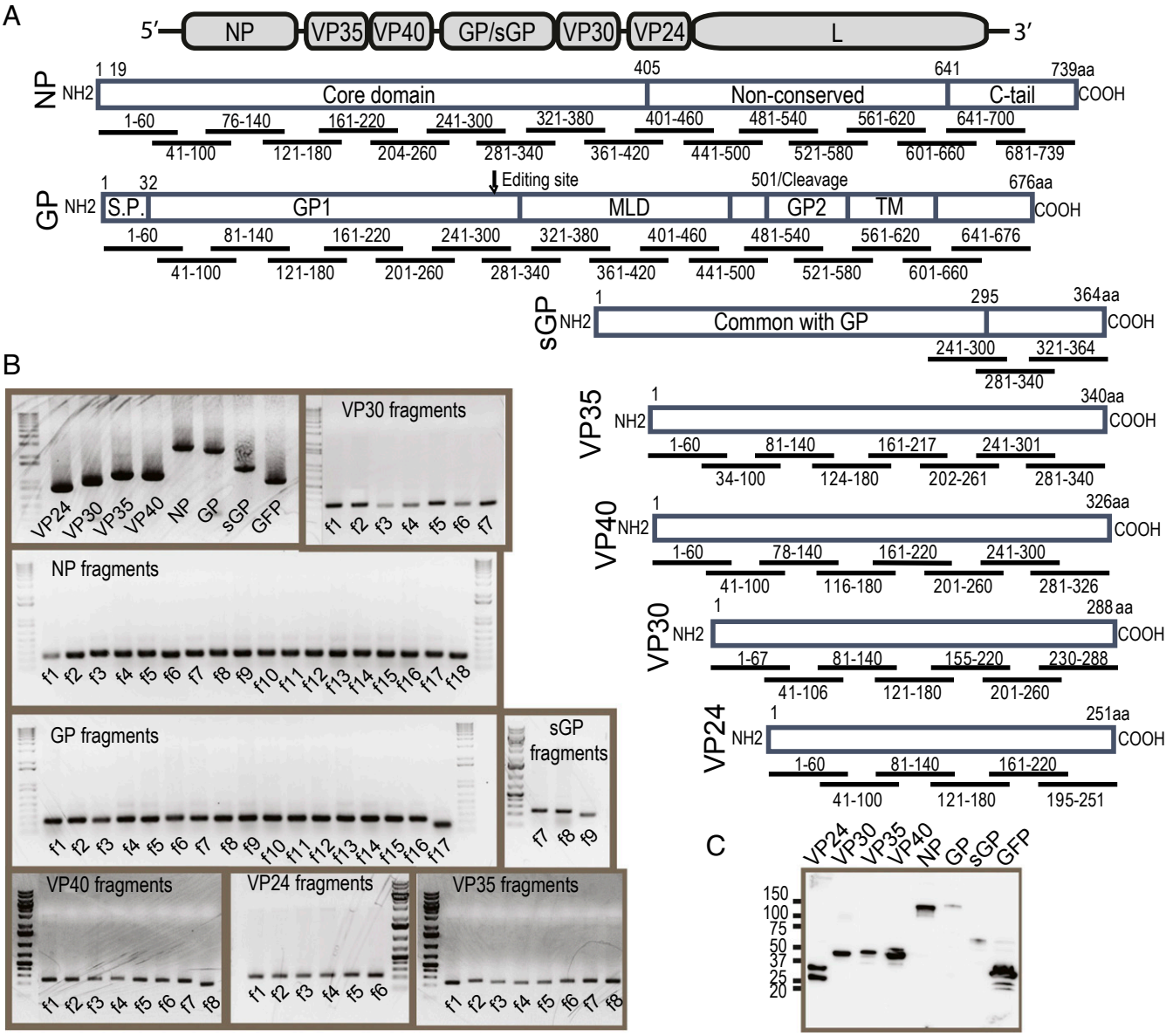

Fig. 1. rscVSVs library for T cell epitope identification in EV. (*A*) Schematic of EBOV proteins and fragments used for the generation of rscVSVs library. EBOV proteins and fragments were based on the sequence of Makona G3845 strain. EBOV genes and genetic fragments were amplified and inserted into pVSVΔG-FLAG vector. (*B*) The rscVSVs were rescued using reverse genetics procedures and plaque-purified. RNA from BHK-21 cells infected with rscVSVs encoding EBOV full-length proteins and fragments was reverse-transcribed into cDNA using oligo dT. Specific cDNAs were then amplified using EBOV gene-specific and flag-specific primers. (*C*) EBOV protein expression from BHK-21 cells infected with rscVSVs was determined by Western blotting using an anti-flag antibody.

HLA typing from 32 Sierra Leonean EVD survivors with confirmed clinical EBOV infections during the 2013–2016 West African outbreak.

Results

rVSVs Encoding for EBOV Proteins Can Stimulate EBOV-Specific Memory CD8$^+$ T Cell Responses in EVD Survivors. To investigate the specificity of EBOV memory T cells, we generated a collection of recombinant single-cycle VSV (rscVSV) (22), each encoding one of seven of the eight proteins expressed by the Makona G3845 isolate of EBOV (2, 23–25) (Fig. 1*A*). The Makona EBOV strain was the cause of the 2013–2016 West African outbreak and highly related to the strains present during the first recorded outbreak of EBOV that occurred decades earlier in Zaire, central Africa (23–26). We rescued 67 additional rscVSVs encoding truncated forms of viral proteins of 36–67 aa for the purpose of defining T cell epitopes in EBOV proteins (Fig. 1). We confirmed mRNA (Fig. 1*B*) and protein (Fig. 1*C*) expression in cells infected with rscVSV expressing all full-length EBOV genes, whereas we characterized rscVSV expressing truncated EBOV gene products based only on mRNA expression (Fig. 1*B*). We isolated peripheral blood mononuclear cells (PBMCs) from 32 individuals (29% male; 71% female; age range: 15–53 y; mean/median age: 33.9/33 y) with a clinical history of EVD. These individuals live in or around the Kenema district of Sierra Leone. Anti-EBOV GP titers were assessed (*SI Appendix*, Fig. S1). Subjects were considered eligible for inclusion if they were registered with the National Ebola Association as having been discharged with a confirmed diagnosis from an Ebola treatment unit. Individuals studied were registered and examined at the Kenema Government Hospital in Kenema, Sierra Leone (26). This study was approved by the Human Subjects Committees of the Broad Institute, The Scripps Research Institute, Tulane University's Human Research Protection Program, and the Sierra Leone Ethics and Scientific Review Committee. Viable PBMCs were incubated with rscVSV/EBOV encoding full-length EBOV genes for 4 h before addition of brefeldin A (4 μg/mL). After overnight culture, CD8$^+$ T cells were assessed for intracellular levels of IFN-γ, TNF-α, and IL-2 by flow cytometry. IL-2 intracellular levels were typically the weakest, thus IFN-γ and TNF-α levels are shown. Samples that exhibited EBOV-specific CD8$^+$ T cell responses were used in subsequent assays with rscVSVs encoding truncated forms of EBOV genes to identify the genetic regions containing T cell epitopes.

We detected EBOV-specific CD8$^+$ T cell responses in 26 of 32 individuals tested for seven EBOV proteins (Fig. 2*A*). EBOV-responsive CD8$^+$ T cells were defined as those samples positive for two of the three cytokines tested, with double-positive cells showing a minimum of one $\log_{10}$ increase of mean fluorescence intensity over both unstimulated and rscVSV-eGFP–stimulated T cells. Two of 32 individuals had background activation, making their CD8$^+$ T cell responses unreliable, while four individuals failed to respond and were left out of the CD8$^+$ T cell analysis (Fig. 2*A*).

NP- and GP-Specific Memory CD8$^+$ T Cell Responses in EVD Survivors. Using the criteria above, 25 of 26 (96%) individuals responded to NP. Of these 25 responders to NP, the NP elicited the strongest and most abundant CD8$^+$ T cell response in 14 individuals. We detected robust EBOV-specific CD8$^+$ T cell responses to VP24 (20 of 26: 77%), VP40 (18 of 26: 69%), and VP35 (11 of 26: 42%) (Fig. 2*A*). Only a minority of responding individuals (10 of 26: 38%) who controlled and cleared EBOV made virus-specific CD8$^+$ T cells to either EBOV GP, sGP, or both (Fig. 2 *A* and *B*). We did not detect VP30-specific CD8$^+$ T cells in any of the individuals studied (0 of 26). Fig. 2*C* shows the percentage of CD8$^+$ T cells expressing both IFN-γ and TNF-α for 30 survivors (excluding the two individuals with high background activation

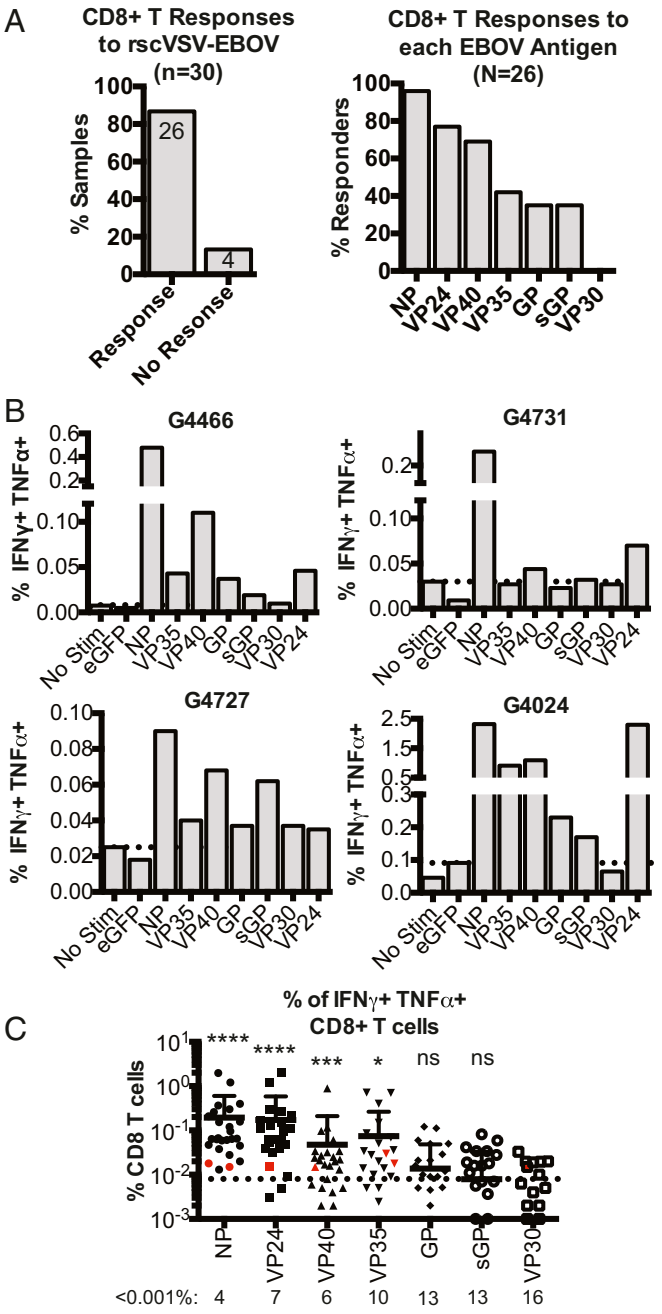

Fig. 2. CD8$^+$ T cell response to EBOV proteins in humans. PBMCs from 32 EVD survivors living in Sierra Leone were infected (MOI = 15) with rscVSVs encoding full-length EBOV proteins. At 4 h postinfection, brefeldin A (4 μg/mL) was added, and PBMCs incubated for 16 h at 37 °C in 5% CO_2. Then CD8$^+$ T cells were assessed for intracellular levels of IFN-γ, TNF-α, and IL-2 by flow cytometry. (*A*, *Left*) Of the 32 individuals studied, two subjects had indeterminate CD8$^+$ T cell responses and were excluded from the analysis. Of the remaining 30 individuals, the percentage of those with CD8$^+$ T cell responses to at least one EBOV protein is shown. (*B*, *Right*) Of the 26 responders, the percentage of individuals whose T cells responded to each EBOV protein is shown. The frequencies of IFN-γ$^+$/TNF-α$^+$ CD8$^+$ T cells of representative survivors (G4036, G4466, G4727, G4731, and G4024) to each EBOV. (*C*) The frequency of IFN-γ$^+$/TNF-α$^+$ CD8$^+$ T cells above the negative control value from 30 individuals is shown. For each subject, the higher negative control value from either unstimulated or rscVSV-GFP was used. Symbols in red show results (>0.001%) from the four nonresponders. The two subjects with indeterminant responses were not included in this analysis. Wilcoxon test comparing each group to VP30 was performed (****$P < 0.0001$, ***$P < 0.001$, *$P < 0.02$, ns, not significant).

but including the four survivors with no detectable responses). These results revealed that responses to NP and VP24 dominated EBOV-specific T cell responses. Eight of 10 individuals that responded to GP or sGP responded to both, suggesting that epitopes may be preferentially located within the conserved sequence between GP and sGP or that multiple epitopes span both proteins. Furthermore, of those that had GP/sGP responses, fewer $CD8^+$ T cells responded to GP or sGP than to other EBOV gene products in the same individual. Individuals who made $CD8^+$ T cell responses to VP24, VP40, and VP35 typically made responses to EBOV NP (Figs. 2–4).

Identification of Epitopes Within the NP Using rscVSVs Encoding for Overlapping Polypeptides Derived from NP Sequences. We then asked whether NP-specific $CD8^+$ T cell epitopes were preferentially present in specific regions within the NP. We used PBMCs from individuals who responded to NP to assess their $CD8^+$ T cell responses to rscVSVs encoding overlapping fragments of NP. This approach presents EBOV peptides to $CD8^+$ T cells in the context of a viral infection, which faithfully recreates the natural processing and loading of peptides onto MHC complexes. By this means, we reduced potential false-positive results associated with other methods that rely primarily on peptide–MHC binding interactions. Epitopes identified are deduced from the overlapping regions of rscVSV encoding for NP fragments that trigger T cell responses. For samples that responded to rscVSVs encoding for a single NP fragment without adjoining fragments triggering responses, we deduced minimal epitope-containing regions as the nonoverlapping region plus 7-aa upstream and 7-aa downstream into overlapping sequences. The 34 epitopes discovered in this study are listed in Table 1 and deposited in the Immune Epitope Database (IEDB).

As an example, PBMCs from individual G4466 made a strong $CD8^+$ T cell response to EBOV NP, while fewer $CD8^+$ T cells responded to VP40, VP24, VP35, GP, and sGP (Fig. 3 *A* and *C*). Furthermore, when incubating PBMCs from G4466 with rscVSVs encoding for ~60-aa overlapping fragments of NP, most T cells responded to NP fragments 1 and 2 (Fig. 3*B*), which identified the overlapping region from $NP_{41–61}$ as the major contributor to $CD8^+$ T cell responses in this individual. A weaker T cell response to NP f3, f4, and f17 occurred, suggesting that $NP_{121–141}$ and $NP_{654–689}$ likely also contribute to NP-specific responses. When this approach was repeated with samples from 13 additional individuals, epitopes were present throughout the NP but with a slight skew toward the N-terminal third of the protein (Fig. 3*D*). Eleven of the 14 individuals responded to one or more of the first six fragments of NP.

Weaker GP Responses Are Skewed Toward the Common Sequence Between GP and sGP. We performed a similar analysis of samples from individuals that responded to GP, sGP, or both. The percent of $CD8^+$ T cells specific to GP/sGP was low compared with NP responses. Individual S-018 exhibited a $CD8^+$ T cell response against GP f3 and sGP f9 that corresponded to $GP/sGP_{94–127}$ and $sGP_{334–364}$, respectively (Fig. 4). This finding illustrates the existence of weak GP responses that are skewed toward regions common between GP and sGP or regions restricted to sGP sequences. Fine epitope mapping of $CD8^+$ T cell epitopes within GP and sGP will reveal whether sGP dominates the GP/sGP response. Our study found that of the 10 individuals

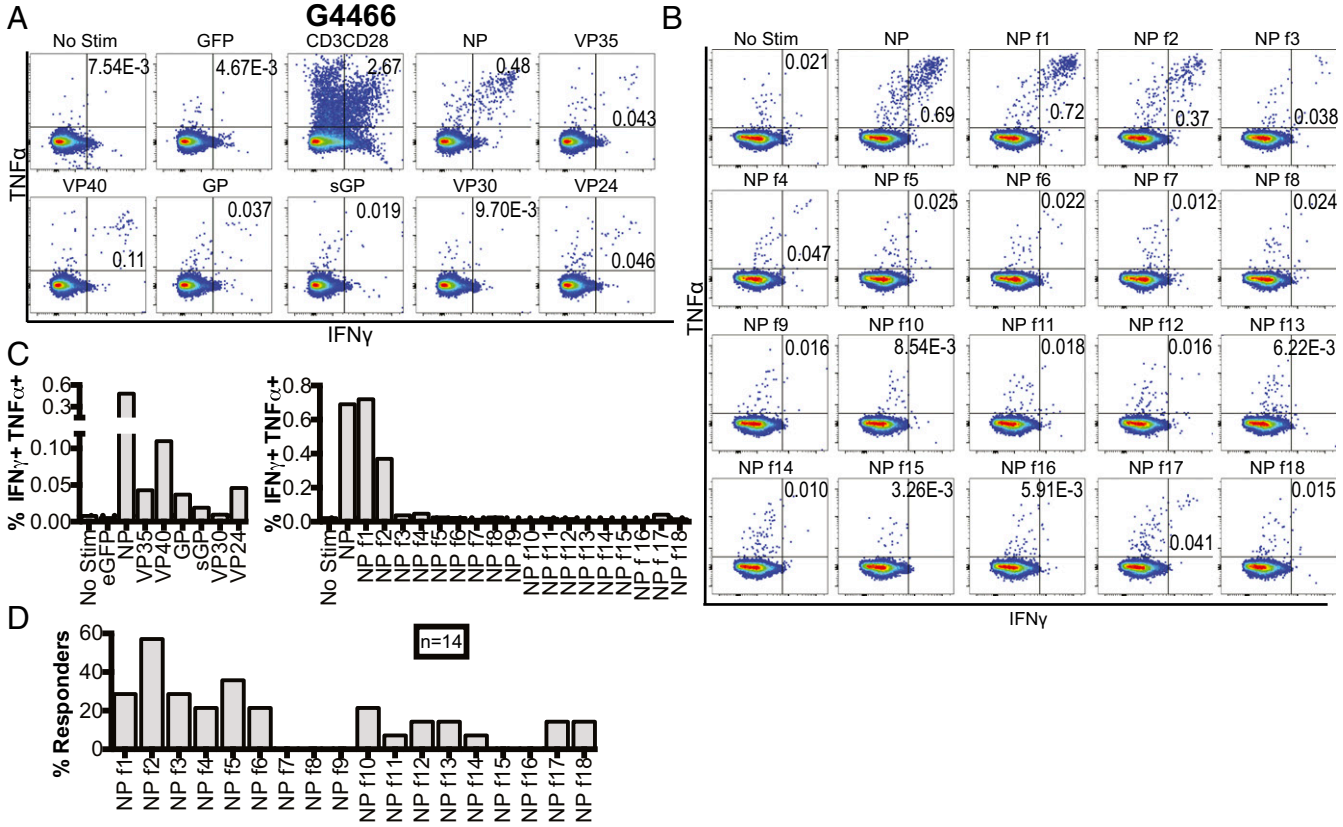

Fig. 3. NP-specific $CD8^+$ T cell responses in EVD survivor G4466. $CD8^+$ T cell response to EBOV full-length proteins (*A*) and NP fragments consist of 59–65 aa overlapping with each other (*B*) were evaluated by intracellular staining of IFN-γ, TNF-α, and IL-2 by flow cytometry (the results of IFN-γ and TNF-α are shown). The frequencies of $IFN\text{-}\gamma^+/TNF\text{-}\alpha^+$ $CD8^+$ T cells are shown in *C*. (*D*) PBMCs from 14 survivors were tested for overlapping fragments from NP. The percentage of responders to each NP fragment is shown.

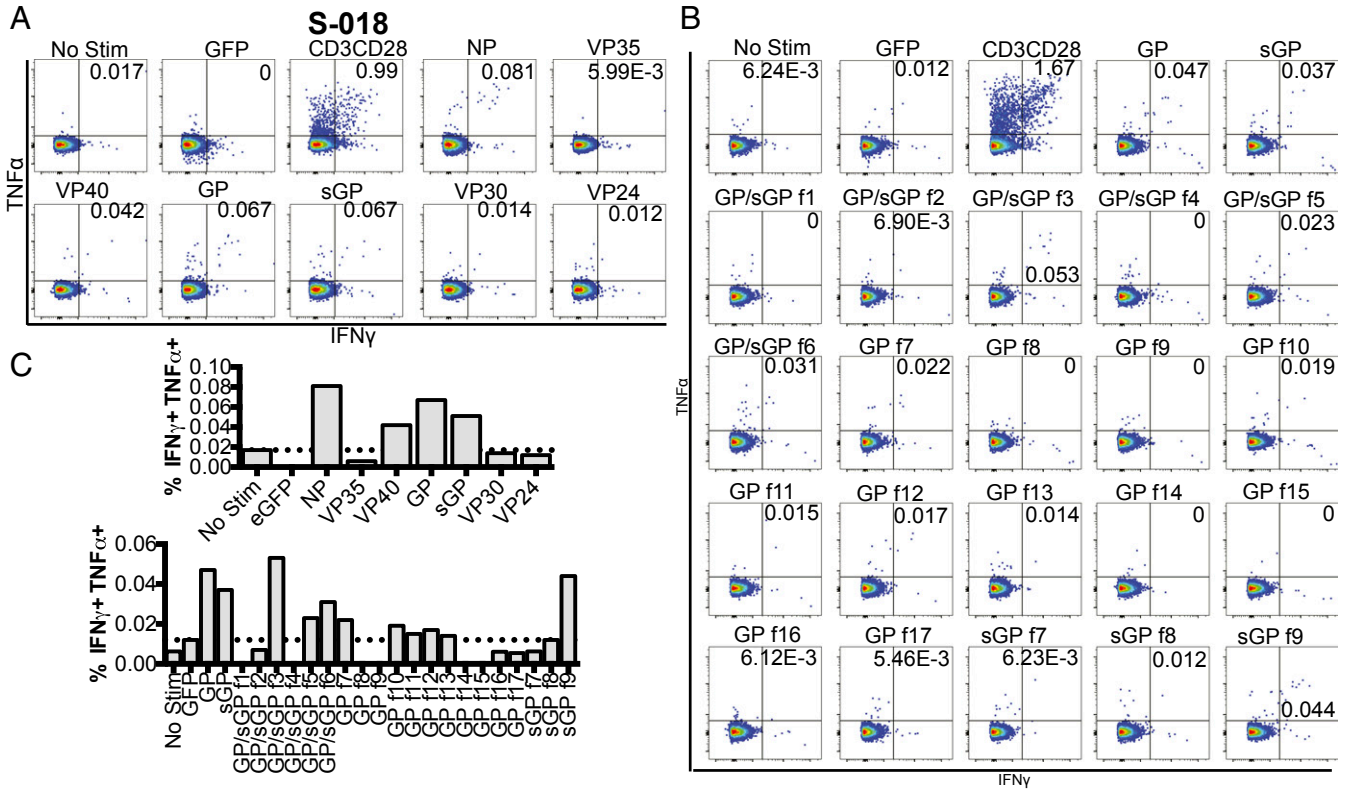

Fig. 4. GP- and sGP-specific CD8$^+$ T cell responses in EVD survivor S-018. CD8$^+$ T cell response to EBOV full-length proteins (*A*) and GP and sGP fragments consist of 36–60 aa overlapping with each other (*B*) were evaluated by intracellular staining of IFN-γ, TNF-α, and IL-2 by flow cytometry (the results of IFN-γ and TNF-α are shown). The frequencies of IFN-γ+/TNF-α+ CD8+ T cells are shown in *C*.

who responded to GP or sGP, only 1 responded to GP and not sGP, despite sGP encoding for 46% less amino acids than GP.

Epitopes 10 aa in Length Were Identified Using a Combination of MHC Binding Prediction and Results from Stimulation with rscVSV. Because T cell responses and epitope presentation are driven by HLA expression, we typed the MHC class I loci of 32 individuals in this study using Illumina's TruSight HLA Sequencing Panels. We found 62 unique alleles among the 192 sequenced (*SI Appendix*, Table S1). With the exception of C*17:01:01, most frequent alleles corresponded to common well-documented alleles, suggesting that epitopes discovered in this study are likely not restricted to the Sierra Leonean Mende population, but applicable to a global population (*SI Appendix*, Table S2). *SI Appendix*, Table S3 lists the three most common epitopes in our study and the HLA alleles expressed by the individuals from which these epitopes were discovered. HLA allelic data has been submitted to the IEDB.

Using epitope data combined with HLA data from individuals from whom epitopes were discovered, we identified smaller 10-aa EBOV epitopes. CD8$^+$ T cell responses to V24, VP35, NP, and VP40 were elicited in PBMCs from EVD survivor S-039 (Fig. 5 *A* and *C*). PBMCs from S-039 were stimulated with rscVSVs encoding overlapping polypeptides from VP24, which resulted in the identification of VP24$_{195–220}$ as the major contributor to VP24-specific responses in this individual (Fig. 5 *B* and *C*). Using the MHC class I binding prediction tools (27–38) from the IEDB (www.iedb.org/) (39), we matched the HLA profile from S-039 and the amino acid sequence VP24$_{195–220}$ and experimentally tested the top four predicted 10-aa epitopes. Only VP24$_{197–206}$ with a predicted restriction to HLA A*74:01 gave a positive result (Fig. 5*D*). Using this method, we discovered 11 additional 10-aa epitopes (*SI Appendix*, Fig. S2). For all 10-aa epitopes listed in Table 1, PBMCs reacted to rscVSVs encoding for whole antigen and the ∼60 polypeptides that contained the 10-aa epitopes. We did not list the larger deduced epitopes if the epitope was subsequently narrowed down to 10 aa. PBMCs from four individuals reacted to VP24$_{66–75}$ (Table 1 and *SI Appendix*, Fig. S2), despite the lack of a common HLA between them (*SI Appendix*, Table S3). Using MHC-I binding prediction tools, this sequence most likely binds one of four HLA B alleles: B*07:06, B*07:02, B*42:01, or B*53:01 [using methods artificial neural network (ANN), stabilized matrix method (SMM), and NetMHCpan, percentile rank ≤ 2.0] (*SI Appendix*, Table S4). Work to experimentally identify the HLA restriction is ongoing.

Discussion

In summary, we used an experimental biological approach that presents EBOV antigens to T cells in a manner that retains endogenous processing and presentation. This method identified epitopes using a combination of rscVSVs, HLA determination, and peptide prediction tools to generate an analysis of memory CD8$^+$ T cell responses in the largest cohort of West African EVD survivors studied thus far. We chose to deliver antigens to antigen presenting cells (APCs) in lieu of identifying epitopes through predicted peptide matrices for several reasons. First, HLAs from the Mende population prevalent in our Sierra Leone cohort have not been well defined, and thus, MHC–peptide binding prediction programs may not have accurately captured the breadth of T cell responses to EBOV antigens. Moreover, to try to understand the breadth of T cell responses in each survivor, costly custom peptide pools would have to be generated for each individual. Second, using VSVs to deliver EBOV whole antigens to determine T cell responses is unbiased, independent

Table 1. EBOV CD8$^+$ T cell epitopes

Epitope position	Amino acid sequence	No. of subjects with epitope
NP 41–60	IPVYQVNNLEEICQLIIQAF	4
NP 54–81	QLIIQAFEAGVDFQESADSFLLMLCLHHA	3
NP 76–100	MLCLHHAYQGDYKLFLESGAVKYLE	1
NP 121–140	LPAVSSGRNIKRTLAAMPEE	1
NP 161–180	LVVGEKACLEKVQRQIQVHA	1
NP 174–210	RQIQVHAEQGLIQYPTAWQSVGHMMVIFRLMRTNFLI	2
NP 178–187	VHAEQGLIQY	1
NP 214–247	LIHQGMHMVAGHDANDAVISNSVAQARFSGLLIV	1
NP 294–227	APFARLLNLSGVNNLEHGLFPQLSAIALGVATAH	1
NP 388–397	FQQTNAMVTL	1
NP 374–420	KILMNFHQKKNEISFQQTNAMVTLRKERLAKLTEAITAASLPKTSGH	1
NP 441–487	HQDDDPTDSQDTTIPDVVVDPDDGGYGEYQSYSENGMSAPDDLVLFD	1
NP 481–500	DDLVLFDLDEDDEDTKPVPN	2
NP 535–544	RTIHHASAPL	1
NP 654–689	HILRSQGPFDAVLYYHMMKDEPVVFSTSDGKEYTYP	2
NP 694–739	EEYPPWLTEKEAMNDENRFVTLDGQQFYWPVMNHRNKFMAILQHHQ	1
NP 706–715	MNDENRFVTL	1
NP 726–735	NHRNKFMAIL	1
VP24 1–47	MAKATGRYNLISPKKDLEKGVVLSDLCNFLVSQTIQGWKVYWAGIEF	1
VP24 41–60	YWAGIEFDVTHKGMALLHRL	1
VP24 66–75	APAWSMTRNL	4
VP24 76–85	FPHLFQNPNS	1
VP24 81–100	QNPNSTIESPLWALRVILAA	1
VP24 134–167	FNMRTQRVKEQLSLKMLSLIRSNILKFINKLDAL	1
VP24 167–176	LHVVNYNGLL	1
VP24 192–201	RTNMGFLVEL	1
VP24 197–206	FLVELQEPDK	1
VP35 94–130	ATVVQQQTIASESLEQRITSLENGLKPVYDMAKTISS	1
VP35 95–104	TVVQQQTIAS	1
VP35 112–121	TSLENGLKPV	1
VP35 134–167	VCAEMVAKYDLLVMTTGRATATAAATEAYWAEHG	1
GP 214–247	YSTTIRYQATGFGTNETEYLFEVDNLTYVQLESR	1
GP 93–127	PPKVVNYEAGEWAENCYNLEIKKPDGSECLPAAPD	1
sGP 334–364	QQMKTTKSWLQKIPLQWFKCTVKEGKLQCRI	1

of in silico prediction, and reliant on the biological processes of viral antigen delivery, endogenous processing, and peptide presentation. Finally, our own experience defining epitopes using peptide pool matrices has led to high false-positive rates, perhaps due to predicted peptide epitopes selected to binding certain HLAs but that would not normally be processed and presented. Nevertheless, we have found that MHC–peptide binding prediction programs accurately predict peptides when used in combination with individualized HLA typing and data from which we have deduced larger epitope regions.

Sixty amino acid polypeptides encoded by rscVSVs induced CD8$^+$ T cell responses similar to those from whole antigens, despite our inability to detect protein by Western blot. This indicated that these polypeptides are likely unstable and quickly degraded. Larger epitopes were deduced from these data. For epitopes that were obtained from CD8$^+$ T cell responses to two adjacent and overlapping 60-aa polypeptides, we considered the percentage and magnitude of the response to decide whether the epitope was present in the overlapping region or whether two distinct epitopes were present. In addition, for CD8$^+$ T cells responding to a 60-aa region without responding to neighboring regions, we chose to define these larger epitopes as those encompassing the nonoverlapping regions with the addition of 7 aa on either side of overlapping regions. This would encompass most epitopes that have anchor residues spaced 7 aa or less. Although unlikely, epitopes may have been missed with this definition.

We identified 12 epitopes of 10 aa each, demonstrating that a combination of viral antigen delivery with MHC–peptide binding prediction was a suitable method for epitope discovery. It was important to reduce potential false-positive results that can accompany predicted peptide matrices as we were constrained to 20 mL of blood or less per individual. Constraints reinforced the need to use the biological rather than chemical strategy to map CD8$^+$ T cell epitopes. Low-level EBOV-specific CD8$^+$ T cell (subdominant epitopes) responses may not be detected with our methodology, as we did not have sufficient PBMCs for continued stimulation and CD8$^+$ T cell expansion. Despite this limitation, additional data from undetected low-level responses would likely not change our conclusions on the dominant NP composition of the EBOV-specific CD8$^+$ T cell memory response in our study population.

In conclusion, we documented the specificity of memory CD8$^+$ T cells generated in an endemic African cohort after a primary EBOV infection. The EBOV-specific memory CD8$^+$ T cells identified include those that responded to EBOV GP and NP. The response to NP was dominant and found in 96% of those with EBOV responses. A strong NP response was anticipated, as the NP gene is positioned at the 5′ end of the EBOV genome and is made in abundance in infected cells. However, the low incidence (38% of EBOV responders) and poor anti-GP CD8$^+$ T cell response was not anticipated. CD8$^+$ T cells specific to EBOV GP and sGP, which together consist of the largest viral protein tested and whose gene is not located at the carboxyl-terminal end of the EBOV genome, were detected less often and with lower activity than T cells specific to other EBOV gene products, except for VP30. T cells specific to epitopes present in

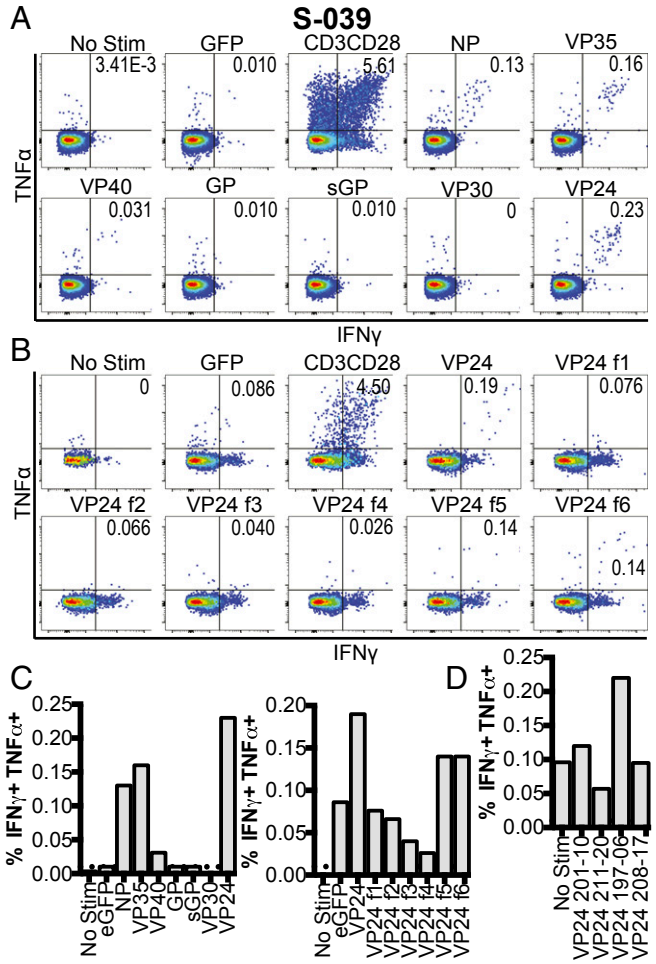

Fig. 5. Identification of CD8$^+$ T cell epitope in VP24 in EVD survivor S-039. CD8$^+$ T cell response to EBOV full-length proteins (*A*) and VP24 fragments consist of 57- to 60-aa polypeptides with 20-aa overlapping regions (*B*) were evaluated by intracellular staining of IFN-γ, TNF-α, and IL-2 by flow cytometry (the results of IFN-γ and TNF-α are shown). The frequencies of IFN-γ$^+$/TNF-α$^+$ CD8$^+$ T cells are shown in *C*. (*D*) PBMCs of EBOV survivor S-039 were incubated with the peptides of predicted epitopes (10 μg/mL) consists of 10 aa in the overlapping region of VP24 f5 and f6 for 1 h. After brefeldin A was added, the PBMCs were incubated for an additional 4 h. Then CD8$^+$ T cells were assessed for intracellular levels of IFN-γ, TNF-α, and IL-2 by flow cytometry. The frequencies of IFN-γ$^+$/TNF-α$^+$ CD8$^+$ T cells are shown.

VP24, which lies closer to the 3′ end of the EBOV genome than GP, were abundant and detected in the majority of EBOV responders (77%). As noted, 10 individuals responded to GP/sGP, with 8 individuals responding to both. GP/sGP share the same amino-terminal 295 residues after which viral polymerase stuttering results in a frameshift mutation so that unique carboxyl-terminal residues occur that differentiate these two viral proteins (381 vs. 69 differential amino acids between GP and sGP, respectively). PBMCs from only one individual responded to GP and not sGP. Identified GP/sGP epitopes were skewed toward the N-terminal half of GP shared with sGP, suggesting that sGP may be more immunogenic than GP.

Based on the observations recorded here, a vaccine designed to elicit both humoral and cellular immunity should minimally include the GP and NP as immunogens. Boosting cellular immunity may have the added advantage of increasing postexposure prophylaxis by providing the optimal cytotoxic T lymphocyte response necessary for clearing acute EBOV infections. Potentially, GP and NP T cell epitopes could be expressed in the context of a string-of-beads–like vaccine (40, 41). With the ability to map peptide epitopes in conjunction with HLA expression, tetramers are under construction that should prove valuable in selected individuals for dissecting EVD pathogenesis in terms of immunity, memory, and virus reactivation.

Materials and Methods

Subjects. Subjects were recruited with the assistance of senior members of the National Ebola Survivors Association. All subjects have a documented clinical history of Ebola infection and were registered with the National Ebola Survivor Association as survivors. Twenty-seven of 32 individuals in this study were also assessed for EBOV-specific antibodies (*SI Appendix*, Fig. S1). The five individuals without EBOV antibody information (but with a clinical history of EVD) consisted of three subjects with measurable CD8$^+$ T cell responses, one without a measurable response, and one with an indeterminate response due to background T cell activation. Our study was approved by the Human Subjects Committees of the Broad Institute, The Scripps Research Institute, Tulane University's Human Research Protection Program, and the Sierra Leone Ethics and Scientific Review Committee. All subjects provided written consent.

PBMC Isolation. Blood collection and PBMC isolation was performed in the Lassa Laboratory at the Kenema Government Hospital (Kenema, Sierra Leone). Blood was diluted with two to three times the volume of PBS and layered on Ficoll-Paque (Fisher). After centrifugation at 400 × *g* at room temperature without brake, the mononuclear cell layer was transferred to a new tube and washed two times with PBS. Isolated PBMCs were suspended with RPMI medium 1640 (Gibco) containing 10% DMSO and 20% FCS, slowly frozen in a −80 °C freezer, shipped to the United States in dry-ice or a liquid-nitrogen dry shipper, and stored in liquid nitrogen until used for T cell assays.

rscVSV Preparation. rscVSVs encoding Ebola virus (Makona G3845) full-length proteins (NP, GP, sGP, VP24, VP30, VP35, and VP40) and their fragments (36–67 aa) were prepared by the method described by Whitt and colleagues (22, 42). Briefly, viral DNA of each protein were amplified by PCR with gene-specific oligonucleotides and then inserted into the pVSV-ΔG-FLAG plasmid. This plasmid contains flag sequences at C-terminus region of the inserted gene. Viruses were rescued, amplified, and purified as described previously (42). Purified viruses were resuspended with RPMI medium 1640 and titrated by plaque assay using BHK-21 cells transfected with VSV-G–expressing plasmid.

RT-PCR. BHK-21 cells were infected with rscVSVs encoding Ebola proteins. At 6 h postinfection, the cells were lysed with TRI reagent (Molecular Research Center), and then BCP phase separation reagent [Molecular Research Center; (10:1)] was added. The cells were mixed and centrifuged for 15 min at 12,000 × *g* at 4 °C. The resulting aqueous layer was mixed with isopropanol and stored for 10 min at room temperature. After centrifugation for 8 min at room temperature, RNA pellet was washed with 75% ethanol, and dissolved with double-distilled water. Isolated RNA was reverse-transcribed with oligonucleotide dT and SuperScript IV reverse transcriptase (Invitrogen). Then PCR was conducted with Ebola gene- (for the forward primer) and flag gene- (for the reverse primer) specific oligonucleotides using GoTaq (Fisher).

Western Blotting. BHK-21 cells were infected with rscVSVs encoding Ebola proteins. At 8 h postinfection, the cells were lysed with Lysis Buffer [50 mM Tris·HCl (pH 7.4), 150 mM NaCl, and 0.5% Nonidet P-40], and mixed with 4× sample buffer. Samples were loaded on precast 4–20% SDS/PAGE gels (Bio-Rad Laboratories). Proteins were transferred electrophoretically to PDVF membrane (Millipore) in transfer buffer (100 mM Tris, 190 mM glycine, and 10% methanol). The membrane was blocked for 30 min at room temperature with TBS containing 0.05% Tween-20 (TBS-T) containing 5% skim milk, and then incubated with anti-flag rabbit polyclonal antibody (1:1,000; Cayman Chemical Company) overnight at 4 °C. After being washed three times with TBS-T, the membrane was incubated with anti-rabbit secondary antibody conjugated with horseradish peroxidase (1:1,000; Pierce) for 1 h at room temperature. After three more washes with TBS-T, proteins were detected using SuperSignal West Pico Chemiluminescent Substrate (Thermo) and visualized by LAS-4000 system (GE Healthcare Life Sciences).

T Cell Assay. PBMCs isolated from EBOV antibody-positive EVD survivors were infected with rscVSVs encoding full-length or fragments of EBOV proteins and GFP at a multiplicity of infection (MOI) of 15. Anti-human CD3 (OKT-3) (60 μg/mL) and CD28 (9.3) (20 μg/mL) antibodies were used as a positive control. At 4 h postinfection, brefeldin A was added (final concentration

4 μg/mL), and PBMCs were incubated for 16 h at 37 °C in 5% CO_2. After removal of the medium, PBMCs were incubated with anti-human Brilliant violet 421 CD4 (RPA-T4) (BioLegend) and FITC CD8a (HIT8a) (BioLegend) for 1 h at 4 °C. After being washed two times with FACS buffer (PBS containing 2% FCS and 0.2% Azide), PBMCs were fixed and permeabilized with BD Cytofix/Cytoperm (BD Biosciences) for 20 min at 4 °C. Following wash two times with BD Perm/Wash (BD Biosciences), PBMCs were stained with anti-human PE TNF-α (BD Biosciences), PE/Cy7 IFN-γ (4S.B3) (BD Biosciences), and APC IL-2 (MQ1-17H12) (BD Biosciences) antibodies for 1 h at 4 °C. Then PBMCs were washed two more times with BD Perm/Wash and suspended with FACS buffer. Flow cytometry was performed using a LSR II (Becton Dickinson), and analyzed with FlowJo software (TreeStar). Peptide stimulations were performed similarly, except 10 μg/mL (unpurified; Anaspec) was added to PBMC cultures. After 1 h, brefeldin A was added and cultures were incubated for an additional 4 h at 37 °C in 5% CO_2.

HLA Typing.

Samples. Genomic DNA from PBMC was extracted from 32 Ebola patients using the Quick DNA Miniprep Plus Kit (Zymo Research), according to the manufacturer's instructions. One reference DNA sample, IHW09263, from the HLA reference panels obtained from the International Histocompatibility Working Group was used as a control for library preparation, data quality, and HLA genotype assignment (Research Cell Bank, Fred Hutchinson Cancer Research Center, Seattle, WA). Sample DNA quality was assessed on a 0.8% agarose gel and DNA concentrations were measured using a Qubit fluorometer (Life Technologies).

PCR amplification and library preparation. Long-range PCR amplification and library preparation was performed using the Illumina TruSight HLA v2 Sequencing Panel, according to the manufacturer's protocols (Illumina). Next, 50 ng of genomic DNA was used for PCR amplification for each of the HLA class I loci. PCR amplicons (HLA-A, 4.1 kb; HLA-B, 2.8 kb; HLA-C, 4.2 kb) were visualized on a 0.8% agarose gel before library preparation. For each sample, HLA PCR amplicons were purified, fragmented, and pooled into one single barcoded library. Final libraries were pooled and subsequently sequenced using the Illumina MiSeq platform.

Sample analysis. The demultiplexed FASTQ data generated by the MiSeq system was uploaded into the TruSight HLA Assign software (v2.1 RUO) for alignment of sample consensus sequences and subsequently compared with the International ImMunoGeneTics Information System/HLA database (v3.26) for HLA genotype determination. HLA allele frequencies were determined by direct count of the number of each allele observed; homozygous alleles were counted twice.

MHC class I binding prediction. Sequences from deduced epitopes identified through rscVSV induced $CD8^+$ T cell responses along with HLA typing from the corresponding individual was input into the MHC-I Binding Predictions tool (v2013-02-22) at the IEDB website (www.iedb.org). IEDB recommended prediction settings were used consisting of Consensus (ANN, SMM, and CombLib) and NetMHCpan. All peptides below the 2% prediction cut-off were tested. If fewer than three predicted peptide epitopes were under this cut-off, we experimentally tested the top three predicted peptide epitopes.

Specific Anti-EBOV GP Determination. The recombinant Ebola IgG ELISA utilizes microwell plates coated with a mixture of recombinant EBOV GP complex. The reference, controls, and patient serum are diluted 1:100 in sample buffer. Diluted reference, controls, and samples are transferred into the microwell plate (100 μL per well) and incubated for 30 min at ambient temperature (18–30 °C). Microwells are washed four times with 300 μL per well of PBS-Tween wash solution. Peroxidase labeled human IgG Fc-specific caprine polyclonal reagent (Jackson ImmunoResearch Laboratories) is added to the microwells (100 μL per well) and incubated at ambient temperature for 30 min. The microwell wash step is repeated. A similar TMB substrate incubation is performed followed by addition of stop solution (100 uL per well). Microplates are read at 450 nm with 650-nm subtraction. All samples are run in duplicate as are a set of six calibrators run in threefold dilutions. Four-parameter logistic regression is performed to standardize the results across plates. The ReLASV IgG assay negative cut-off is 2.5 SDs above the interpolated value of the average negative control.

ACKNOWLEDGMENTS. We thank the Ebola Survivors Association for their time, effort, and sacrifice in helping us better understand this deadly disease. The authors are funded by National Institute of Allergy and Infectious Diseases's Large Scale T Cell Epitope Discovery Contract HHSN272201400048C under BAA-NIAID-DAIT-NIHAI2013167.

1. Hofman M, Au S (2017) *The Politics of Fear: Médecins Sans Frontières and the West African Ebola Epidemic* (Oxford Univ Press, New York).
2. Oldstone MBA, Oldstone MR (2017) *Ebola's Curse: 2013-2016 Outbreak in West Africa* (Academic, London).
3. Cross RW, et al. (2016) Analytical validation of the ReEBOV antigen rapid test for point-of-care diagnosis of Ebola virus infection. *J Infect Dis* 214(Suppl 3):S210–S217.
4. Boisen ML, et al. (2016) Field validation of the ReEBOV antigen rapid test for point-of-care diagnosis of Ebola virus infection. *J Infect Dis* 214(Suppl 3):S203–S209.
5. Broadhurst MJ, et al. (2015) ReEBOV antigen rapid test kit for point-of-care and laboratory-based testing for Ebola virus disease: A field validation study. *Lancet* 386: 867–874.
6. Davey RT, Jr, et al.; PREVAIL II Writing Group; Multi-National PREVAIL II Study Team (2016) A randomized, controlled trial of ZMapp for Ebola virus infection. *N Engl J Med* 375:1448–1456.
7. Siegel D, et al. (2017) Discovery and synthesis of a phosphoramidate prodrug of a pyrrolo[2,1-f][triazin-4-amino] adenine C-nucleoside (GS-5734) for the treatment of Ebola and emerging viruses. *J Med Chem* 60:1648–1661.
8. Kraft CS, et al.; Nebraska Biocontainment Unit and the Emory Serious Communicable Diseases Unit (2015) The use of TKM-100802 and convalescent plasma in 2 patients with Ebola virus disease in the United States. *Clin Infect Dis* 61:496–502.
9. Boisen ML, et al. (2016) Epidemiology and management of the 2013-16 West African Ebola outbreak. *Annu Rev Virol* 3:147–171.
10. Henao-Restrepo AM, et al. (2015) Efficacy and effectiveness of an rVSV-vectored vaccine expressing Ebola surface glycoprotein: Interim results from the Guinea ring vaccination cluster-randomised trial. *Lancet* 386:857–866.
11. Warfield KL, et al. (2015) Homologous and heterologous protection of nonhuman primates by Ebola and Sudan virus-like particles. *PLoS One* 10:e0118881.
12. Feldmann H, Sanchez A, Geisbert TW (2007) Filoviridae: Marburg and Ebola viruses. *Fields Virology*, eds Knipe DM, Howley PM (Lippincott Williams & Wilkins, Philadelphia), 5th Ed, pp 1409–1448.
13. Centers for Disease Control and Prevention (2018) Years of Ebola virus disease outbreaks. Available at https://www.cdc.gov/vhf/ebola/history/chronology.html. Accessed May 30, 2018.
14. McElroy AK, et al. (2015) Human Ebola virus infection results in substantial immune activation. *Proc Natl Acad Sci USA* 112:4719–4724.
15. Baize S, et al. (1999) Defective humoral responses and extensive intravascular apoptosis are associated with fatal outcome in Ebola virus-infected patients. *Nat Med* 5: 423–426.
16. Zinkernagel RM, Althage A (1977) Antiviral protection by virus-immune cytotoxic T cells: Infected target cells are lysed before infectious virus progeny is assembled. *J Exp Med* 145:644–651.
17. Oldstone MB (1994) The role of cytotoxic T lymphocytes in infectious disease: History, criteria, and state of the art. *Curr Top Microbiol Immunol* 189:1–8.
18. Sullivan NJ, et al. (2011) CD8+ cellular immunity mediates rAd5 vaccine protection against Ebola virus infection of nonhuman primates. *Nat Med* 17:1128–1131.
19. Oswald WB, et al. (2007) Neutralizing antibody fails to impact the course of Ebola virus infection in monkeys. *PLoS Pathog* 3:e9.
20. Marzi A, et al. (2013) Antibodies are necessary for rVSV/ZEBOV-GP-mediated protection against lethal Ebola virus challenge in nonhuman primates. *Proc Natl Acad Sci USA* 110:1893–1898.
21. McElroy AK, et al. (2016) Kinetic analysis of biomarkers in a cohort of US patients with Ebola virus disease. *Clin Infect Dis* 63:460–467.
22. Moseley NB, et al. (2012) Use of replication restricted recombinant vesicular stomatitis virus vectors for detection of antigen-specific T cells. *J Immunol Methods* 375: 118–128.
23. Gire SK, et al. (2014) Genomic surveillance elucidates Ebola virus origin and transmission during the 2014 outbreak. *Science* 345:1369–1372.
24. Holmes EC, Dudas G, Rambaut A, Andersen KG (2016) The evolution of Ebola virus: Insights from the 2013-2016 epidemic. *Nature* 538:193–200.
25. Park DJ, et al. (2015) Ebola virus epidemiology, transmission, and evolution during seven months in Sierra Leone. *Cell* 161:1516–1526.
26. Goba A, et al.; Viral Hemorrhagic Fever Consortium (2016) An outbreak of Ebola virus disease in the Lassa fever zone. *J Infect Dis* 214(Suppl 3):S110–S121.
27. Andreatta M, Nielsen M (2016) Gapped sequence alignment using artificial neural networks: Application to the MHC class I system. *Bioinformatics* 32:511–517.
28. Lundegaard C, et al. (2008) NetMHC-3.0: Accurate web accessible predictions of human, mouse and monkey MHC class I affinities for peptides of length 8-11. *Nucleic Acids Res* 36:W509–W512.
29. Lundegaard C, Nielsen M, Lund O (2006) The validity of predicted T-cell epitopes. *Trends Biotechnol* 24:537–538.
30. Lundegaard C, Lund O, Nielsen M (2008) Accurate approximation method for prediction of class I MHC affinities for peptides of length 8, 10 and 11 using prediction tools trained on 9mers. *Bioinformatics* 24:1397–1398.
31. Nielsen M, et al. (2003) Reliable prediction of T-cell epitopes using neural networks with novel sequence representations. *Protein Sci* 12:1007–1017.
32. Buus S, et al. (2003) Sensitive quantitative predictions of peptide-MHC binding by a 'Query by Committee' artificial neural network approach. *Tissue Antigens* 62: 378–384.
33. Peters B, Sette A (2005) Generating quantitative models describing the sequence specificity of biological processes with the stabilized matrix method. *BMC Bioinformatics* 6:132.

34. Sidney J, et al. (2008) Quantitative peptide binding motifs for 19 human and mouse MHC class I molecules derived using positional scanning combinatorial peptide libraries. *Immunome Res* 4:2.
35. Moutaftsi M, et al. (2006) A consensus epitope prediction approach identifies the breadth of murine T(CD8+)-cell responses to vaccinia virus. *Nat Biotechnol* 24:817–819.
36. Nielsen M, Andreatta M (2016) NetMHCpan-3.0; improved prediction of binding to MHC class I molecules integrating information from multiple receptor and peptide length datasets. *Genome Med* 8:33.
37. Hoof I, et al. (2009) NetMHCpan, a method for MHC class I binding prediction beyond humans. *Immunogenetics* 61:1–13.
38. Nielsen M, et al. (2007) NetMHCpan, a method for quantitative predictions of peptide binding to any HLA-A and -B locus protein of known sequence. *PLoS One* 2:e796.
39. Vita R, et al. (2015) The Immune Epitope Database (IEDB) 3.0. *Nucleic Acids Res* 43: D405–D412.
40. Whitton JL, Sheng N, Oldstone MB, McKee TA (1993) A "string-of-beads" vaccine, comprising linked minigenes, confers protection from lethal-dose virus challenge. *J Virol* 67:348–352.
41. Oldstone MB, Tishon A, Geckeler R, Lewicki H, Whitton JL (1992) A common antiviral cytotoxic T-lymphocyte epitope for diverse major histocompatibility complex haplotypes: Implications for vaccination. *Proc Natl Acad Sci USA* 89: 2752–2755.
42. Whitt MA (2010) Generation of VSV pseudotypes using recombinant ΔG-VSV for studies on virus entry, identification of entry inhibitors, and immune responses to vaccines. *J Virol Methods* 169:365–374.